

Therapeutic Effects of Microbubbles Added to Combined High-Intensity Focused Ultrasound and Chemotherapy in a Pancreatic Cancer Xenograft Model

Mi Hye Yu, MD¹, Jae Young Lee, MD, PhD², Hae Ri Kim³, Bo Ram Kim², Eun-Joo Park, PhD²,
Hoe Suk Kim, PhD², Joon Koo Han, MD, PhD², Byung Ihn Choi, MD, PhD⁴

¹Department of Radiology, Konkuk University Medical Center, Seoul 05030, Korea; ²Department of Radiology, Seoul National University Hospital, Seoul 03080, Korea; ³Department of Pre-Dentistry, Gangneung-Wonju National University College of Dentistry, Gangneung 25457, Korea; ⁴Department of Radiology, Chung-Ang University Hospital, Seoul 06973, Korea

Objective: To investigate whether high-intensity focused ultrasound (HIFU) combined with microbubbles enhances the therapeutic effects of chemotherapy.

Materials and Methods: A pancreatic cancer xenograft model was established using BALB/c nude mice and luciferase-expressing human pancreatic cancer cells. Mice were randomly assigned to five groups according to treatment: control (n = 10), gemcitabine alone (GEM; n = 12), HIFU with microbubbles (HIFU + MB, n = 11), combined HIFU and gemcitabine (HIGEM; n = 12), and HIGEM + MB (n = 13). After three weekly treatments, apoptosis rates were evaluated using the terminal deoxynucleotidyl transferase-mediated dUTP nick end-labeling assay in two mice per group. Tumor volume and bioluminescence were monitored using high-resolution 3D ultrasound imaging and *in vivo* bioluminescence imaging for eight weeks in the remaining mice.

Results: The HIGEM + MB group showed significantly higher apoptosis rates than the other groups ($p < 0.05$) and exhibited the slowest tumor growth. From week 5, the tumor-volume-ratio relative to the baseline tumor volume was significantly lower in the HIGEM + MB group than in the control, GEM, and HIFU + MB groups ($p < 0.05$). Despite visible distinction, the HIGEM and HIGEM + MB groups showed no significant differences.

Conclusion: High-intensity focused ultrasound combined with microbubbles enhances the therapeutic effects of gemcitabine chemotherapy in a pancreatic cancer xenograft model.

Keywords: Microbubbles; High-intensity focused ultrasound; Pancreatic cancer; Gemcitabine; Sonoporation; Animal study

Received February 22, 2016; accepted after revision June 15, 2016.

This research was supported by a Basic Science Research Program through the National Research Foundation of Korea (NRF) funded by the Ministry of Science, ICT & Future Planning (2012R1A1A1010930) and by the MSIP (Ministry of Science, ICT and Future Planning), Korea, under the C-ITRC (Convergence Information Technology Research Center) support program (NIPA-2014-H0401-14-1002) supervised by the NIPA (National IT Industry Promotion Agency). This research was also supported by Grant No. 04-2013-1090 from the SNUH Research Fund.

Corresponding author: Jae Young Lee, MD, PhD, Department of Radiology, Seoul National University Hospital, 101 Daehak-ro, Jongno-gu, Seoul 03080, Korea.

• Tel: (822) 2072-3073 • Fax: (822) 743-6385
• E-mail: leejy4u@snu.ac.kr

This is an Open Access article distributed under the terms of the Creative Commons Attribution Non-Commercial License (<http://creativecommons.org/licenses/by-nc/3.0>) which permits unrestricted non-commercial use, distribution, and reproduction in any medium, provided the original work is properly cited.

INTRODUCTION

Pancreatic cancer has poor prognosis since the majority are not treatable by surgery at the time of diagnosis because the cancer is often locally advanced or metastatic (1, 2). Therefore, many patients with untreatable pancreatic cancer undergo palliative systemic chemotherapy or concurrent chemoradiotherapy (3). To date, many first-line chemotherapeutic agents, including gemcitabine, have been used to increase the overall survival of patients with advanced pancreatic cancer (4-6). However, the results of chemotherapy are still disappointing, showing < 10% 5-year overall survival rate over the last decade (7). Therefore, there is a clinical need to enhance chemotherapeutic results in pancreatic cancer.

High-intensity focused ultrasound (HIFU) is an emerging

therapeutic technique that uses ultrasound waves as carriers of energy. It permits non-invasive treatment of benign and malignant solid tumors, including pancreatic cancer (8-10). In the past decade, several preclinical and clinical studies demonstrated that HIFU is safe and effective for local tumor control and palliative pain control in advanced pancreatic cancer (9-14). Moreover, concurrent treatment with HIFU and gemcitabine shows promising results in advanced pancreatic cancer (15, 16).

Microbubbles are a widely used ultrasound contrast agent that has recently received widespread attention for sonoporation. Sonoporation is a transient increase in cell membrane permeability by the use of ultrasound alone or ultrasound with microbubbles (17-19). It enhances intracellular uptake of drugs and genes (20-22). When microbubbles are exposed to ultrasound in a vessel, they oscillate and act as cavitation nuclei; and these oscillations lead to an increase in the membrane permeability of surrounding epithelial cells (21-23). Ultrasound alone increases cell membrane permeability (24), however, the presence of microbubbles augments membrane permeability to a greater extent (25-27). Recent *in vitro* studies demonstrated that ultrasound with microbubbles can increase cell permeability to chemotherapeutic drugs, decrease cell viability, and consequently increase chemotherapeutic efficacy against tumor cells (28, 29).

Kotopoulos et al. (30, 31) suggested combining ultrasound with microbubbles and gemcitabine as a novel modality for enhanced drug delivery in pancreatic cancer. Ultrasound combined with microbubbles and gemcitabine extends the treatment period in pancreatic cancer patients compared with control patients (30) and improves inhibition of tumors in a pancreatic xenograft model, as compared with gemcitabine alone (31). Only three groups (control, gemcitabine, and ultrasound combined with microbubbles and gemcitabine) were compared in the study, and thus, there was no comparative data related to the additional therapeutic effect of microbubbles on the combination of ultrasound and gemcitabine. In this study, we compared the difference between HIFU combined with microbubbles and chemotherapy versus HIFU combined with chemotherapy alone using a pancreatic cancer animal model.

Therefore, the purpose of this study was to investigate whether HIFU combined with microbubbles enhances the effects of chemotherapy in a pancreatic cancer xenograft model.

MATERIALS AND METHODS

This animal study was approved by our Institutional Animal Care Use Committee (IACUC No. 13-0254).

Pancreatic Cancer Cell Preparation and Mouse Xenograft Model Development

Human pancreatic cancer cells (PANC-1) infected with lentivirus and the luciferase gene were cultured for bioluminescence imaging. High luciferase-expressing cells were selected with puromycin (2.5 µg/mL) and cultured in Dulbecco's modified Eagle's medium containing 10% fetal bovine serum and 1% penicillin. After digestion with 0.25% trypsin at 37°C, the pancreas cancer cell lines were mixed (1:1) with Matrigel (Becton Dickinson, Frankling Lakes, NJ, USA), and the cell concentration was adjusted to 5×10^6 /mL with normal saline.

BALB/c male nude mice weighing between 25 and 35 g were used for a xenograft model. The BALB/c nude mice were inoculated with 0.2 mL cell suspension in the subcutaneous layer at the same level of the unilateral flank using a sterile syringe. Three weeks after inoculation, the tumors were visualized using high-resolution 3D ultrasound (Vevo2100®, VisualSonics Inc., Ontario, Canada) and bioluminescence imaging (IVIS® Lumina II, PerkinElmer Inc., Waltham, MA, USA).

HIFU Equipment and Treatment Parameters

A pre-clinical HIFU system (VIFU 2000®, Alpinion Medical Systems, Seoul, Korea) was used for ultrasound treatment (Fig. 1) (32). The therapeutic transducer is a 1.1-MHz single element spherical-focused transducer with a central circular opening of 40 mm in diameter. HIFU exposure was performed in a tank that was filled with degassed water, which was controlled at a degassing level of ≤ 4 ppm and a temperature of 36.0°C. Prior to HIFU treatment, intraperitoneal general anesthesia was administered using a mixture of 30 mg/kg zolazepam (Zoletil®, Virbac, Carros, France) and 10 mg/kg xylazine hydrochloride (Rompun 2%, Bayer Korea, Seoul, Korea). The tumor-bearing mice were set in an animal holder, and the target tumor was positioned at the center of the therapeutic transducer's focal zone according to ultrasound guidance (E-CUBE 9®, Alpinion Medical Systems) using a 7-MHz center frequency transducer. The diameter and natural focus of the annular were both 63.2 mm. The focal zone was 1.3 x 1.3 x 9.2 mm with a center frequency of 1.1 MHz at -6 dB. For precise

targeting, the HIFU system was equipped with 3D target position control (x-, y-, and z-axis) with a precision of 0.01 mm and travel speed of 12.5 mm/s. Pulsed HIFU beams insonated the tumor and moved automatically at 2 mm space intervals to cover the entire tumor (Fig. 1). The following acoustic parameters used to treat the pancreatic tumors were determined by reference to a prior study (33) on concurrent HIFU and gemcitabine treatment using a pancreatic xenograft model: frequency, 1.1 MHz; peak negative pressure, 3.2 MPa (mechanical index [MI] = 3.05); pulse repetition frequency, 40 Hz; duty cycle, 50%; treatment duration, 20 seconds.

Treatment Groups

The following five treatment groups were established according to the treatment protocol: control group (no treatment), gemcitabine alone (GEM), HIFU with microbubbles (HIFU + MB), combined HIFU and gemcitabine (HIGEM), and combined HIFU and gemcitabine with microbubbles (HIGEM + MB). Treatment was performed weekly

for three weeks except for the mice in the control group.

In the groups that were treated with a chemotherapeutic drug (i.e., the GEM, HIGEM, and HIGEM + MB groups), 200 mg/kg of gemcitabine (Gemzar®, Eli Lilly Co., Indianapolis, IN, USA) was administered into each mouse intraperitoneally immediately prior to HIFU treatment to maximize the therapeutic effect (33).

In the groups that were treated with microbubbles (i.e., HIFU + MB, HIGEM + MB groups), an ultrasound contrast agent (SonoVue®, Bracco Imaging, S.p.A, Milan, Italy) was used according to the manufacturer's instructions. The microbubbles were prepared immediately prior to the treatment of the first mouse, and the vial was agitated prior to each HIFU treatment to ensure a homogeneous concentration between 1×10^8 - 5×10^8 microbubbles per milliliter (34). A fine cannula was inserted into the tail vein of the mouse using a 31 G fine needle to accurately inject the microbubbles into the vessels of a mouse (Fig. 1). Based on previous studies (31, 35, 36), 0.05 mL of microbubbles was injected immediately before HIFU via the

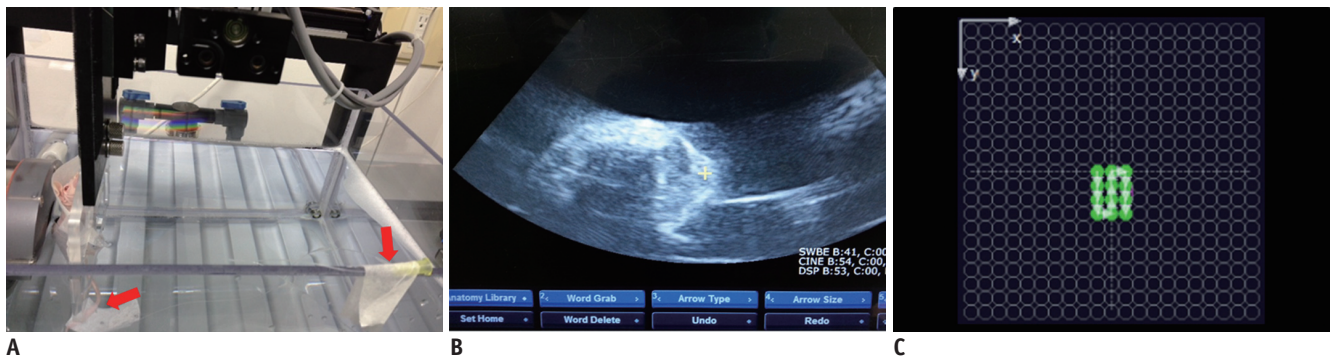


Fig. 1. Pre-clinical high-intensity focused ultrasound (HIFU) system.

A. HIFU treatment was performed in tank filled with degassed water maintained at temperature of 36.0°C, with tumor-bearing mouse set in animal holder. Microbubbles were injected via tail vein catheter (arrows) before HIFU treatment. **B.** Target tumor was positioned at center of therapeutic transducer's focal zone according to ultrasound guidance. **C.** For precise targeting, HIFU system is equipped with three-dimensional target position control (x-, y-, and z-axis). Pulsed HIFU beams are insonated into tumor and cover entire tumor with 2 mm spacing between sonication spots.

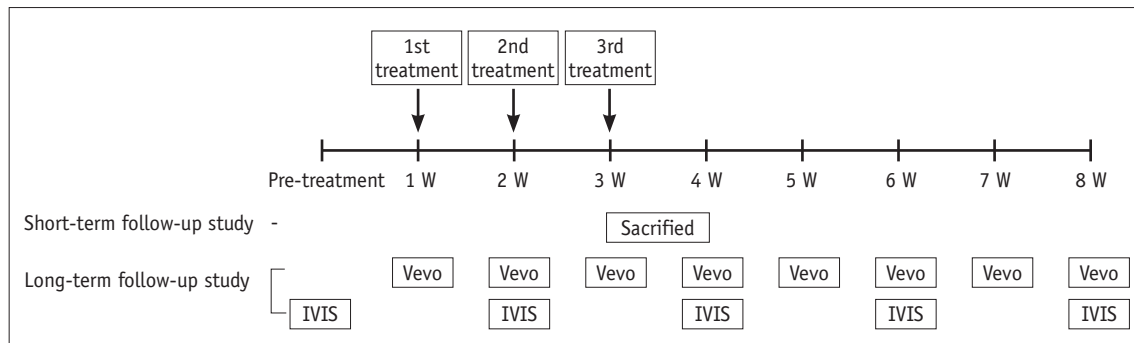


Fig. 2. Flow chart of study design. IVIS = *in vivo* bioluminescence imaging, Vevo = high-resolution three-dimensional ultrasound for tumor volume measurement

tail vein cannula. In the HIGEM + MB group, intraperitoneal injection of gemcitabine, administration of microbubbles, and HIFU treatment were performed in order.

Experimental Protocol

This animal study consisted of two subgroup studies to evaluate the short-term and long-term persistent therapeutic effects after treatment. A flow chart summarizing the study design was presented in Figure 2.

Short-Term Follow-Up Study

Two mice were assigned to each treatment group. The mice were sacrificed for histopathologic evaluation after 48 hours at the end of the last treatment (Fig. 2), as described for identification of cell apoptosis (37). After euthanizing the mice, representative specimens were obtained, and tissue sections (4 μ m) were prepared using a microtome, placed on glass slides and stained with Harris' hematoxylin solution and eosin Y (Sigma, St. Louis, MO, USA). Subsequently, the terminal deoxynucleotidyl transferase-mediated dUTP nick end-labeling (TUNEL) assay was performed to quantify the apoptotic cells using an ApopTag[®] Peroxidase *In Situ* Apoptosis Detection Kit (Millipore, Bedford, MA, USA). Two researchers calculated

the apoptotic rate as the fraction of total number of apoptotic cells among the total number of cancer cells. Each researcher independently counted TUNEL-positive neoplastic cells, defined as brown-stained nuclear or cytoplasmic staining in five randomly selected high-power fields (\times 200 magnification) using Image J software (National Institutes of Health, Bethesda, MD, USA). The resulting 10 values were averaged.

Long-Term Follow-Up Study

A total of 48 mice were randomly allocated into the following five groups: control (n = 8), GEM (n = 10), HIFU + MB (n = 9), HIGEM (n = 10), and HIGEM + MB (n = 11). As in the short-term follow-up study, a total of 3 cycles of treatment were administered to the mice, with the exception of the control mice, weekly for three weeks, followed by a five-week observation period without treatment (Fig. 2). We used high-resolution 3D ultrasonic imaging (A Vevo2100[®], VisualSonics Inc.) to monitor tumor growth and bioluminescence imaging (IVIS[®] Lumina II) for *in vivo* cell imaging. Serial tumor volumes of the mice were measured weekly using a Vevo2100 ultrasound scanner with a MS250 probe (13–24 MHz) for 8 consecutive weeks starting at the beginning of the treatment. Each tumor was scanned using B-mode and 3D mode; and to capture 3D images, the scan was performed under respiratory gating. Then, the 3D images of the tumor were manually contoured along the tumor margin throughout the 3D stack. The tumor volume was automatically measured using parallel segmentation in the Vevo2100 software (version 1.3.0, VisualSonics Inc.) (Fig. 3). The mean volume of the tumors before treatment was 69.5 mm³ (\pm 30.6 mm³). *In vivo* bioluminescence imaging was performed every two weeks for eight weeks (pre-treatment, week 2, 4, 6, and 8). The mice were anesthetized with 2% isoflurane and intraperitoneally injected with 15 mg/mL D-luciferin solution (VivoGlo[®], Luciferin, Promega, WI, USA) 10 minute prior to imaging. The bioluminescence signals were measured as the total photonic count detected within a manual region of interest in the tumor using Living Image software (version 2.50, *In Vivo* Imaging Systems).

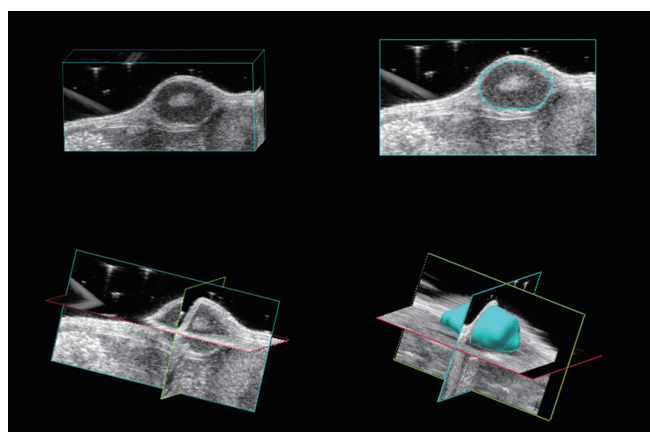


Fig. 3. Tumor volume measurement using high-resolution three-dimensional (3D) ultrasound. Tumors were scanned using 3D mode under respiratory gating. Tumors in captured 3D images were manually contoured along tumor margin. Then, tumor volume was automatically calculated using parallel segmentation in Vevo2100 software.

Table 1. Tumor Apoptosis Rate According to Treatment Group

	Control	GEM	HIFU + MB	HIGEM	HIGEM + MB
Apoptosis rate (% , mean \pm SD)	12.68 \pm 4.02	18.19 \pm 2.44	20.17 \pm 4.32	19.90 \pm 3.15	26.69 \pm 6.58

Values are expressed as mean \pm SD. Control = no treatment, GEM = gemcitabine treatment, HIFU = high-intensity focused ultrasound, HIFU + MB = HIFU with microbubbles treatment, HIGEM = combined HIFU and gemcitabine treatment, HIGEM + MB = combined HIFU and gemcitabine with microbubbles treatment

Statistical Analysis

In the short-term follow-up study, the apoptosis rate was compared among the treatment groups. The results of

the long-term follow-up study were reported as the mean values \pm standard error of mean. To minimize the influence of differences in initial tumor volume among the mice, the

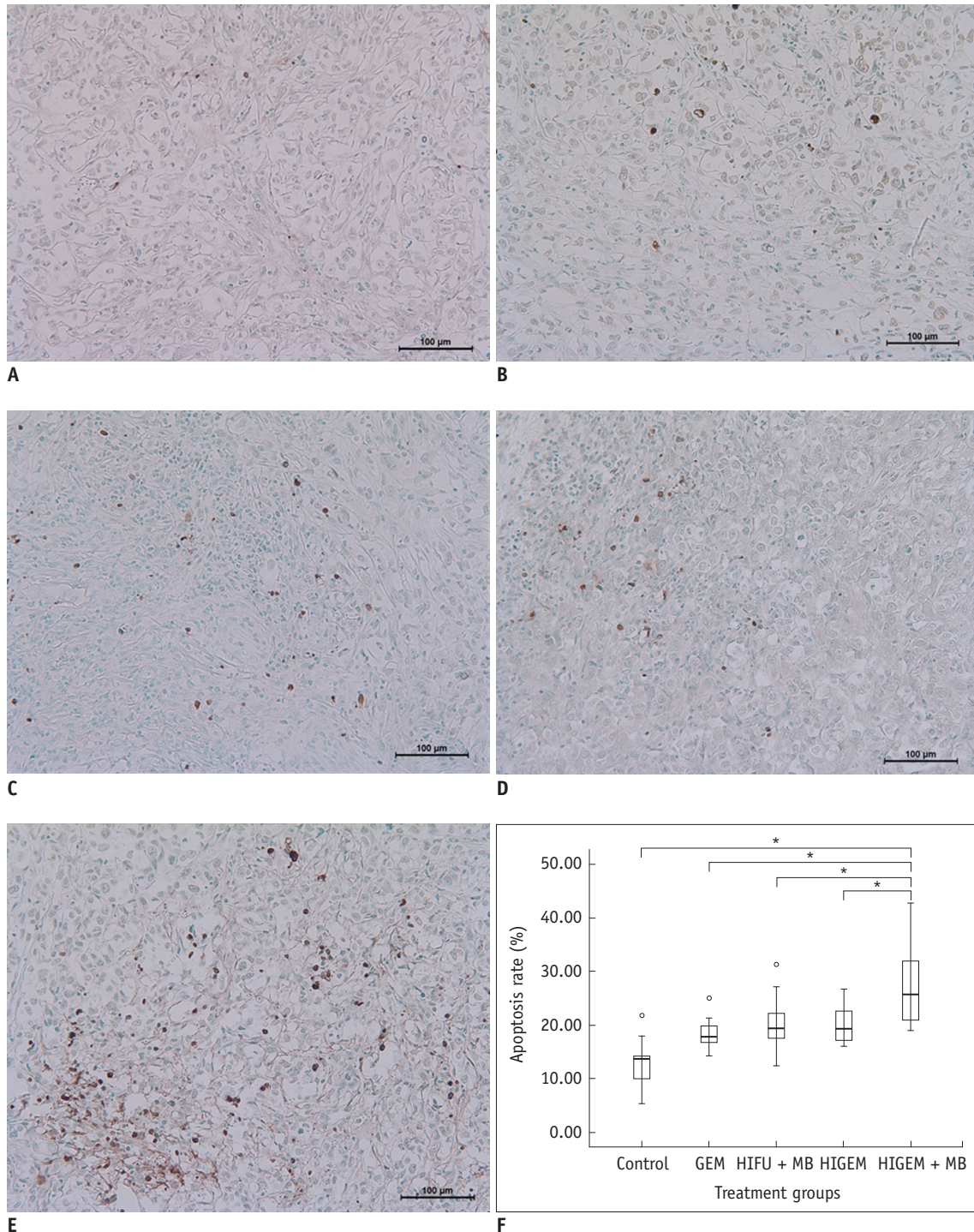


Fig. 4. TUNEL assay results and apoptosis rates according to treatment group.

A-E. Apoptotic cells were quantified using TUNEL assay. TUNEL-positive, brown-stained apoptotic cells were visualized under high-power field (x 200 magnification) in each treatment group: control (**A**), GEM (**B**), HIFU + MB (**C**), HIGEM (**D**), and HIGEM + MB (**E**). **F.** Box and whisker plots of tumor apoptosis in each group. There were significant differences in tumor apoptosis between HIGEM + MB group and control, GEM, HIFU + MB, and HIGEM groups ($p < 0.05$). *Significant difference ($p < 0.05$). Control = no treatment, GEM = gemcitabine treatment alone, HIFU = high-intensity focused ultrasound, HIFU + MB = HIFU with microbubbles treatment, HIGEM = combined HIFU and gemcitabine treatment, HIGEM + MB = combined HIFU and gemcitabine with microbubbles treatment, TUNEL = terminal deoxynucleotidyl transferase-mediated dUTP nick end-labeling

tumor-volume-ratio (i.e., the tumor volume on a specific day divided by the baseline tumor volume) was compared among the groups. Statistical analysis was performed using the Kruskal-Wallis test and the Mann-Whitney test with SPSS (version 17.0, SPSS Inc., Chicago, IL, USA). A p value < 0.05 was considered as statistically significant difference.

RESULTS

Short-Term Follow-Up Study

The TUNEL assay and apoptosis rate in each of the study groups were presented in Table 1 and Figure 4. The HIGEM + MB group showed significantly higher tumor apoptosis rate ($26.69 \pm 6.58\%$), as compared to the other groups ($p < 0.05$). The control group showed a significantly lower apoptosis rate ($12.68 \pm 4.02\%$) than the other groups ($p < 0.05$). Apoptosis rate showed no significant differences between the GEM, HIFU + MB, and HIGEM groups. On histologic evaluation, coagulative necrosis with surrounding congestion, hemorrhage, or inflammatory cell infiltration suggestive of thermal ablation was not observed in any tumors treated with HIFU.

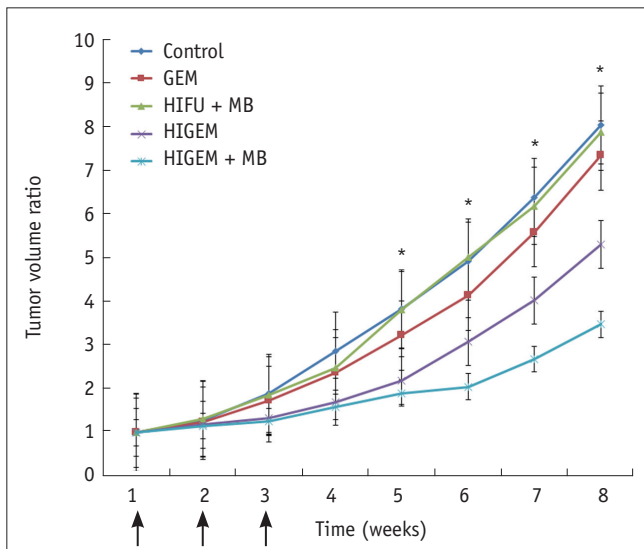


Fig. 5. Tumor volume ratio according to treatment group.

Line graphs demonstrating serial change in tumor-volume-ratio (i.e., tumor volume on specific day divided by baseline tumor volume) in each treatment group. Black arrows indicate treatment days. HIGEM + MB group shows slowest growth rate and most delayed growth spurt among study groups. Significant differences were observed starting in 5th week between HIGEM + MB group and control, GEM, and HIFU + MB groups, respectively. *Significant difference ($p < 0.05$). Control = no treatment, GEM = gemcitabine treatment alone, HIFU = high-intensity focused ultrasound, HIFU + MB = HIFU with microbubbles treatment, HIGEM = combined HIFU and gemcitabine treatment, HIGEM + MB = combined HIFU and gemcitabine with microbubbles treatment

Long-Term Follow-Up Study

Overall, tumor size increased with time in all five treatment groups (Fig. 5). The tumors gradually increased from the beginning in the control group; whereas, the tumors in the other groups were relatively suppressed during the first three weeks (treatment period). Among these groups, the HIGEM + MB group showed the most delayed tumor growth with initiation of rapid tumor growth at the 4th week in the GEM and HIFU + MB groups, at the 5th week in the HIGEM group, and at the 6th week in the HIGEM + MB group.

In addition, tumors in the HIGEM + MB group showed the slowest growth rate among the five groups. Starting in the 5th week, the tumor-volume-ratio in the HIGEM + MB group was significantly lower than those in the control, GEM, and HIFU + MB groups ($p < 0.05$, asterisks in Fig. 5). The HIGEM + MB group was also lower than the HIGEM group in tumor-volume-ratio, without significance ($p > 0.05$). When compared with the control group, the tumor-volume-ratio in the HIGEM + MB group was significantly lower during weeks 3 through 8 (all $p < 0.05$). Meanwhile, the HIGEM group showed a significantly lower tumor-volume-ratio only in the 3rd week ($p = 0.09$).

Through *in vivo* bioluminescence imaging, the total photonic flux after the start of treatment indicated that the HIGEM + MB group tended to have lower bioluminescence than the other groups (Fig. 6). However, a significant difference was not found. During weeks 6 through 8, gross tumor necrosis was observed in several mice with large tumors (control, $n = 4$; GEM, $n = 3$; HIFU + MB, $n = 2$). However, gross tumor necrosis was not observed in the HIGEM and HIGEM + MB groups.

DISCUSSION

Our study results demonstrated that the addition of microbubbles to HIFU had synergistic therapeutic effects with gemcitabine in a pancreatic cancer xenograft model by increasing the apoptosis of tumor cells and likely inhibiting tumor growth. The HIGEM + MB group showed significantly higher apoptosis rate than the HIGEM group. The HIGEM + MB group exhibited slower tumor growth than the HIGEM group during the 8-week study period.

The basic concept and experimental protocol of our study were similar to that of Kotopoulis et al. (31). However, there were several differences between the studies. We used PANC-1 cells as human pancreatic cancer cell line and

a subcutaneous xenograft model; whereas, they used the MIA PaCa-2 cell line and an orthotopic xenograft model. Most importantly, they included only three groups (control,

gemcitabine, and combined ultrasound and gemcitabine with microbubbles) without combined ultrasound and gemcitabine treatment. Consequentially, it is unclear whether the

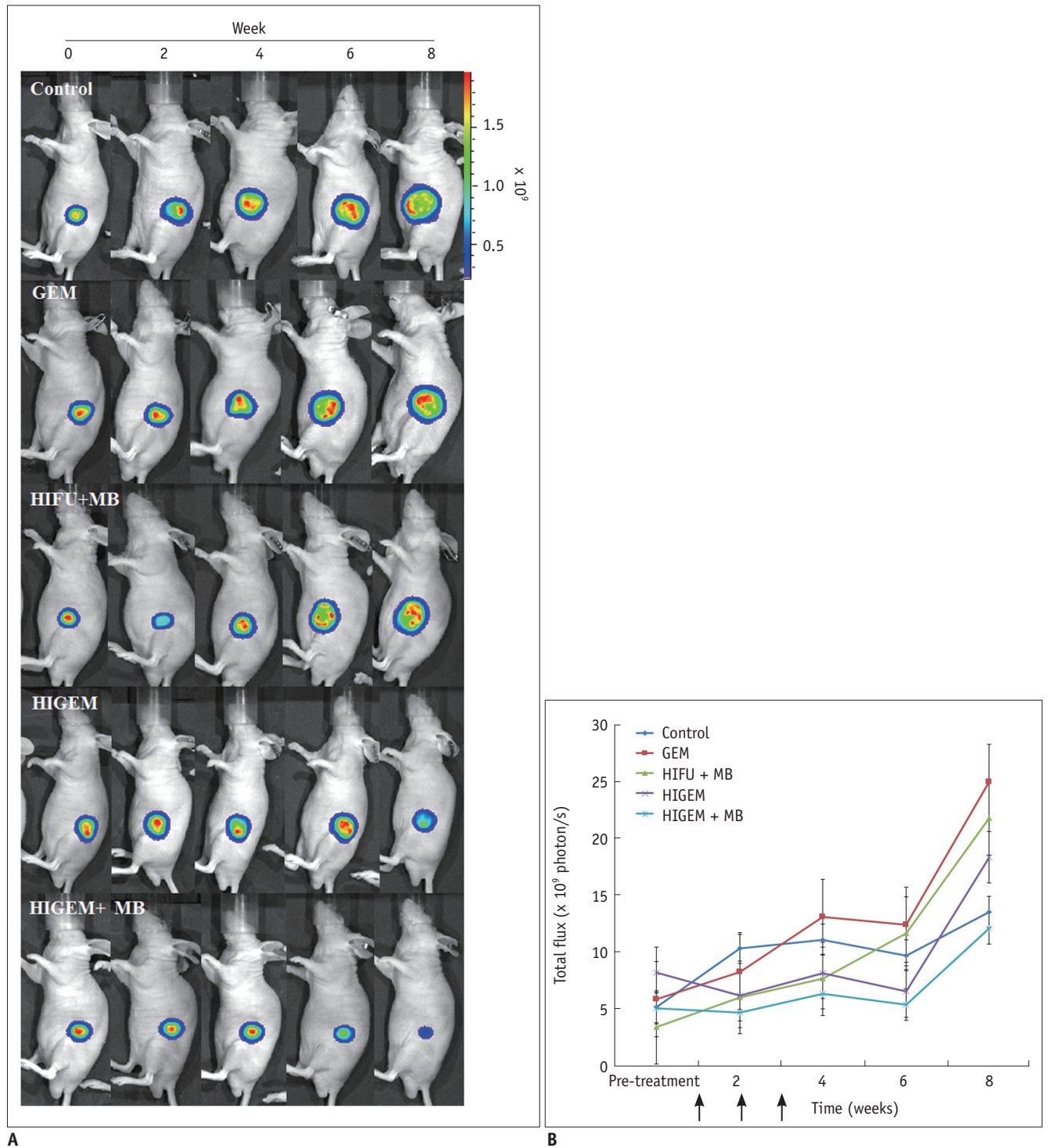


Fig. 6. In vivo bioluminescence imaging in treatment groups.

A. Bioluminescence imaging of representative mouse from each treatment group. HIGEM + MB group shows much lower total photonic flux during 8th week. **B.** Black arrows indicate treatment days. Despite no significant difference between treatment groups, HIGEM + MB group shows lower total photonic flux than other groups. Control = no treatment, GEM = gemcitabine treatment alone, HIFU = high-intensity focused ultrasound, HIFU + MB = HIFU with microbubbles treatment, HIGEM = combined HIFU and gemcitabine treatment, HIGEM + MB = combined HIFU and gemcitabine with microbubbles treatment

enhanced therapeutic effect in their study is due to the addition of the microbubbles or due merely to a synergistic effect of ultrasound and gemcitabine regardless of the microbubbles. In contrast, we found a higher apoptosis rate and more delayed and slower tumor growth rate in the HIGEM + MB group than in the HIGEM group (Fig. 5).

The synergistic therapeutic effects of microbubbles with combined HIFU and chemotherapeutic drugs corroborate the results of prior *in vitro* studies using retinoblastoma cells, colon carcinoma, and murine mammary carcinoma (28, 29). We applied the concept of additional effects of microbubbles to a pancreatic cancer animal model using a relatively large number of mice and a long follow-up period of eight weeks. The tumor growth pattern observed in this study also agrees with a prior study by Lee et al. (33). Tumor growth was relatively suppressed during treatment, followed by a subsequent rapid increase after treatment termination. The five treatment groups revealed different growth curves. The HIGEM + MB group showed the most delayed tumor growth and the slowest tumor growth rate among the five groups. It is likely that differences in tumor-volume-ratio between the HIGEM and HIGEM + MB groups would have been more evident on 8 cycles of continued treatments, as in the study by Kotopoulis et al. (31).

Microbubbles reportedly improve the thermal and cavitation effects of HIFU in several previous animal studies (35, 36, 38-41). However, most of the prior studies performed a single HIFU treatment without use of chemotherapeutic drugs and evaluated only the immediate therapeutic effects (i.e., coagulating volume and cavitory necrosis). In this study, although the HIFU + MB group showed a significantly higher apoptosis rate than the control group, the tumors in the HIFU + MB group showed rapid growth starting in the 4th week, after three cycles of treatment, with a tumor-volume-ratio similar to that of the control group since the 5th week (Fig. 5). Based on our study results, the combination of HIFU and microbubbles in the absence of a chemotherapeutic drug is not therapeutically effective in the long-term. This result also suggests that the enhanced therapeutic effects of the HIGEM + MB treatment mainly results from the enhancement of drug delivery by sonoporation caused by addition of microbubbles and not from the concurrent therapeutic effects of HIFU and microbubbles.

In this study, we used HIFU parameters with pulse repetition frequency, 40 Hz; duty cycle, 50%; peak negative pressure, 3.2 MPa; treatment duration, 20 seconds. These

parameters may not cause gross thermal ablation, since areas of thermal ablation were not observed in any tumors treated with HIFU on histologic evaluation in this study. While it may have thermal effects (42), the mechanical effects of ultrasound were mainly considered in the HIFU conditions of this study (MI = 3.05). Thermal exposure near the ablation threshold (50–60°C) in HIFU can cause cell apoptosis (42-44), hence, the enhanced therapeutic effects of the HIGEM + MB treatment might be partly due to subthreshold thermal exposure, as well as sonoporation.

As a basic study, our study shows the feasibility of HIFU combined with microbubbles to enhance the effects of chemotherapy for pancreatic cancer. However, there are several limitations. Firstly, although the subcutaneous xenograft model is an established animal model (32, 33, 45, 46), in contrast, the human pancreas is located in the deep portion and surrounded with adjacent organs and bowel. In addition, this study was performed under specific sonication settings. There are differences between the animal model and human pancreatic cancer, such as the degree of penetration of the abdominal wall and the possibility of interference from abdominal gas in humans. Therefore, further basic and clinical research is required for the re-optimization of HIFU parameters prior to clinical study. Third, the bioluminescence values in the control group were considerably lower in this study. This can be explained by the hypoxic core in the tumor and tumor necrosis, because they decrease bioluminescence signals. Mice in the control group experienced more hypoxic core and tumor necrosis due to their larger tumor volumes, which resulted in decreased bioluminescence starting in week 4, in contrast to the other groups, which experienced an increase in bioluminescence starting in week 4. Moreover, half of the mice in the control group showed visible tumor necrosis during weeks 6 through 8.

Despite the need for further studies, our study demonstrates promising results in a relatively large number of mice and a long-term follow-up period of eight weeks. In conclusion, the addition of microbubbles may enhance the therapeutic effects of combined HIFU and chemotherapy by increasing cell apoptosis and inhibiting tumor growth, and has potential as an alternative pancreatic cancer treatment in clinics.

REFERENCES

1. von Wichert G, Seufferlein T, Adler G. Palliative treatment of

- pancreatic cancer. *J Dig Dis* 2008;9:1-7
2. Hariharan D, Saied A, Kocher HM. Analysis of mortality rates for pancreatic cancer across the world. *HPB (Oxford)* 2008;10:58-62
 3. Cardenes HR, Chiorean EG, Dewitt J, Schmidt M, Loehrer P. Locally advanced pancreatic cancer: current therapeutic approach. *Oncologist* 2006;11:612-623
 4. Maréchal R, Bachel JB, Mackey JR, Dalban C, Demetter P, Graham K, et al. Levels of gemcitabine transport and metabolism proteins predict survival times of patients treated with gemcitabine for pancreatic adenocarcinoma. *Gastroenterology* 2012;143:664-674.e1-e6
 5. el-Kamar FG, Grossbard ML, Kozuch PS. Metastatic pancreatic cancer: emerging strategies in chemotherapy and palliative care. *Oncologist* 2003;8:18-34
 6. Burris HA 3rd, Moore MJ, Andersen J, Green MR, Rothenberg ML, Modiano MR, et al. Improvements in survival and clinical benefit with gemcitabine as first-line therapy for patients with advanced pancreas cancer: a randomized trial. *J Clin Oncol* 1997;15:2403-2413
 7. Mukherjee S, Hudson E, Reza S, Thomas M, Crosby T, Maughan T. Pancreatic cancer within a UK cancer network with special emphasis on locally advanced non-metastatic pancreatic cancer. *Clin Oncol (R Coll Radiol)* 2008;20:535-540
 8. Orsi F, Arnone P, Chen W, Zhang L. High intensity focused ultrasound ablation: a new therapeutic option for solid tumors. *J Cancer Res Ther* 2010;6:414-420
 9. Jang HJ, Lee JY, Lee DH, Kim WH, Hwang JH. Current and future clinical applications of high-intensity focused ultrasound (HIFU) for pancreatic cancer. *Gut Liver* 2010;4 Suppl 1:S57-S61
 10. Wu F, Wang ZB, Zhu H, Chen WZ, Zou JZ, Bai J, et al. Feasibility of US-guided high-intensity focused ultrasound treatment in patients with advanced pancreatic cancer: initial experience. *Radiology* 2005;236:1034-1040
 11. Xiong LL, Hwang JH, Huang XB, Yao SS, He CJ, Ge XH, et al. Early clinical experience using high intensity focused ultrasound for palliation of inoperable pancreatic cancer. *JOP* 2009;10:123-129
 12. Sofuni A, Moriyasu F, Sano T, Yamada K, Itokawa F, Tsuchiya T, et al. The current potential of high-intensity focused ultrasound for pancreatic carcinoma. *J Hepatobiliary Pancreat Sci* 2011;18:295-303
 13. Sung HY, Jung SE, Cho SH, Zhou K, Han JY, Han ST, et al. Long-term outcome of high-intensity focused ultrasound in advanced pancreatic cancer. *Pancreas* 2011;40:1080-1086
 14. Li PZ, Zhu SH, He W, Zhu LY, Liu SP, Liu Y, et al. High-intensity focused ultrasound treatment for patients with unresectable pancreatic cancer. *Hepatobiliary Pancreat Dis Int* 2012;11:655-660
 15. Zhao H, Yang G, Wang D, Yu X, Zhang Y, Zhu J, et al. Concurrent gemcitabine and high-intensity focused ultrasound therapy in patients with locally advanced pancreatic cancer. *Anticancer Drugs* 2010;21:447-452
 16. Lee JY, Choi BI, Ryu JK, Kim YT, Hwang JH, Kim SH, et al. Concurrent chemotherapy and pulsed high-intensity focused ultrasound therapy for the treatment of unresectable pancreatic cancer: initial experiences. *Korean J Radiol* 2011;12:176-186
 17. Iwanaga K, Tominaga K, Yamamoto K, Habu M, Maeda H, Akifusa S, et al. Local delivery system of cytotoxic agents to tumors by focused sonoporation. *Cancer Gene Ther* 2007;14:354-363
 18. Karshafian R, Bevan PD, Williams R, Samac S, Burns PN. Sonoporation by ultrasound-activated microbubble contrast agents: effect of acoustic exposure parameters on cell membrane permeability and cell viability. *Ultrasound Med Biol* 2009;35:847-860
 19. Bazan-Peregrino M, Arvanitis CD, Rifai B, Seymour LW, Coussios CC. Ultrasound-induced cavitation enhances the delivery and therapeutic efficacy of an oncolytic virus in an in vitro model. *J Control Release* 2012;157:235-242
 20. Kudo N, Okada K, Yamamoto K. Sonoporation by single-shot pulsed ultrasound with microbubbles adjacent to cells. *Biophys J* 2009;96:4866-4876
 21. Tzu-Yin W, Wilson KE, Machtaler S, Willmann JK. Ultrasound and microbubble guided drug delivery: mechanistic understanding and clinical implications. *Curr Pharm Biotechnol* 2013;14:743-752
 22. Delalande A, Kotopoulis S, Postema M, Midoux P, Pichon C. Sonoporation: mechanistic insights and ongoing challenges for gene transfer. *Gene* 2013;525:191-199
 23. Ibsen S, Schutt CE, Esener S. Microbubble-mediated ultrasound therapy: a review of its potential in cancer treatment. *Drug Des Devel Ther* 2013;7:375-388
 24. Lawrie A, Brisken AF, Francis SE, Tayler DI, Chamberlain J, Crossman DC, et al. Ultrasound enhances reporter gene expression after transfection of vascular cells in vitro. *Circulation* 1999;99:2617-2620
 25. Lindner JR. Microbubbles in medical imaging: current applications and future directions. *Nat Rev Drug Discov* 2004;3:527-532
 26. Hernet S, Klibanov AL. Microbubbles in ultrasound-triggered drug and gene delivery. *Adv Drug Deliv Rev* 2008;60:1153-1166
 27. Suzuki R, Oda Y, Utoguchi N, Maruyama K. Progress in the development of ultrasound-mediated gene delivery systems utilizing nano- and microbubbles. *J Control Release* 2011;149:36-41
 28. Watanabe Y, Aoi A, Horie S, Tomita N, Mori S, Morikawa H, et al. Low-intensity ultrasound and microbubbles enhance the antitumor effect of cisplatin. *Cancer Sci* 2008;99:2525-2531
 29. Lee NG, Berry JL, Lee TC, Wang AT, Honowitz S, Murphree AL, et al. Sonoporation enhances chemotherapeutic efficacy in retinoblastoma cells in vitro. *Invest Ophthalmol Vis Sci* 2011;52:3868-3873
 30. Kotopoulis S, Dimcevski G, Gilja OH, Hoem D, Postema M. Treatment of human pancreatic cancer using combined ultrasound, microbubbles, and gemcitabine: a clinical case study. *Med Phys* 2013;40:072902

31. Kotopoulos S, Delalande A, Popa M, Mamaeva V, Dimcevski G, Gilja OH, et al. Sonoporation-enhanced chemotherapy significantly reduces primary tumour burden in an orthotopic pancreatic cancer xenograft. *Mol Imaging Biol* 2014;16:53-62
32. Kim JH, Kim H, Kim YJ, Lee JY, Han JK, Choi BI. Dynamic contrast-enhanced ultrasonographic (DCE-US) assessment of the early response after combined gemcitabine and HIFU with low-power treatment for the mouse xenograft model of human pancreatic cancer. *Eur Radiol* 2014;24:2059-2068
33. Lee ES, Lee JY, Kim H, Choi Y, Park J, Han JK, et al. Pulsed high-intensity focused ultrasound enhances apoptosis of pancreatic cancer xenograft with gemcitabine. *Ultrasound Med Biol* 2013;39:1991-2000
34. Greis C. Technology overview: SonoVue (Bracco, Milan). *Eur Radiol* 2004;14 Suppl 8:P11-P15
35. He W, Wang W, Zhou P, Wang YX, Zhou P, Li RZ, et al. Enhanced ablation of high intensity focused ultrasound with microbubbles: an experimental study on rabbit hepatic VX2 tumors. *Cardiovasc Intervent Radiol* 2011;34:1050-1057
36. Chung DJ, Cho SH, Lee JM, Hahn ST. Effect of microbubble contrast agent during high intensity focused ultrasound ablation on rabbit liver in vivo. *Eur J Radiol* 2012;81:e519-e523
37. Poff JA, Allen CT, Traughber B, Colunga A, Xie J, Chen Z, et al. Pulsed high-intensity focused ultrasound enhances apoptosis and growth inhibition of squamous cell carcinoma xenografts with proteasome inhibitor bortezomib. *Radiology* 2008;248:485-491
38. Yu T, Wang G, Hu K, Ma P, Bai J, Wang Z. A microbubble agent improves the therapeutic efficiency of high intensity focused ultrasound: a rabbit kidney study. *Urol Res* 2004;32:14-19
39. Kaneko Y, Maruyama T, Takegami K, Watanabe T, Mitsui H, Hanajiri K, et al. Use of a microbubble agent to increase the effects of high intensity focused ultrasound on liver tissue. *Eur Radiol* 2005;15:1415-1420
40. Luo W, Zhou X, Ren X, Zheng M, Zhang J, He G. Enhancing effects of SonoVue, a microbubble sonographic contrast agent, on high-intensity focused ultrasound ablation in rabbit livers in vivo. *J Ultrasound Med* 2007;26:469-476
41. Luo W, Zhou X, Zhang J, Qian Y, Zheng M, Yu M, et al. Analysis of apoptosis and cell proliferation after high intensity-focused ultrasound ablation combined with microbubbles in rabbit livers. *Eur J Gastroenterol Hepatol* 2007;19:962-968
42. Vykhodtseva N, McDannold N, Martin H, Bronson RT, Hynynen K. Apoptosis in ultrasound-produced threshold lesions in the rabbit brain. *Ultrasound Med Biol* 2001;27:111-117
43. Kennedy JE, Ter Haar GR, Cranston D. High intensity focused ultrasound: surgery of the future? *Br J Radiol* 2003;76:590-599
44. Hilger I, Rapp A, Greulich KO, Kaiser WA. Assessment of DNA damage in target tumor cells after thermoablation in mice. *Radiology* 2005;237:500-506
45. Casey G, Cashman JP, Morrissey D, Whelan MC, Larkin JO, Soden DM, et al. Sonoporation mediated immunogene therapy of solid tumors. *Ultrasound Med Biol* 2010;36:430-440
46. Jiang L, Hu B, Guo Q, Chen L. Treatment of pancreatic cancer in a nude mouse model using high-intensity focused ultrasound. *Exp Ther Med* 2013;5:39-44